Sborník vědeckých prací Vysoké školy báňské - Technické univerzity Ostrava
číslo 1, rok 2008, ročník VIII, řada stavební
článek č. 8

Miroslav ROSMANIT[1], Monique C. M. BAKKER[2]

ELASTIC POST-BUCKLING BEHAVIOR OF UNIFORMLY COMPRESSED PLATES

Abstract

In this paper it is discussed how existing analytical and semi-analytical formulas for describing the elastic-post-buckling behavior of uniformly compressed square plates with initial imperfections, for loads up to three times the buckling load can be simplified and improved. For loads larger than about twice the buckling load the influence of changes in the buckling shape, assumed sinusoidal, cannot be neglected anymore. These changes can be taken into account by using the perturbation approach. The existing and improved formulas are compared to the results of finite element simulations.

1 INTRODUCTION

In this paper the post-buckling behavior of square plates, as shown in fig. 2. is studied. All edges of the plate are simply supported ($u_z = 0$). The edges loaded by the compression force are forced to remain straight, but free to experience Poisson's contraction. The other two edges are free to wave in-plane, thus membrane stresses in the y-direction are equal to zero. These boundary conditions correspond to the boundary conditions usually used for the modeling of compression flanges in thin-walled steel deck sections. These boundary conditions correspond to the boundary conditions usually used for the modeling of compression flanges. The concentrated load causes deformations of the compression flange which may be quite large [1]. Therefore it was decided to study the behavior of uniformly compressed plates for loads up to three times the buckling load, and for initial imperfections up to two times the plate thickness.

When a perfectly flat simply supported plate is subjected to uniaxial compression, the stress distribution is uniform over the plate, until the buckling load is reached. After buckling the stress distribution becomes non-uniform, both over the width b and the length a of the plate. Plate with unloaded edges forced to remain straight but free to move in-plane have the same buckling load, but differ in their post-buckling behavior, see Fig. 1.

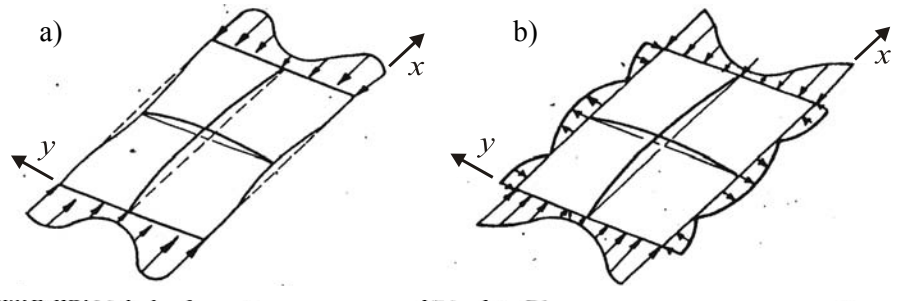

Fig. 1: a) Plate with unloaded edges stress free and able to wave.
b) Plate with all edges kept straight.

[1] Ing. Miroslav Rosmanit, Ph.D., Katedra konstrukcí, Fakulta stavební, VŠB-Technická univerzita Ostrava, Ludvíka Podéště 1875, Ostrava-Poruba, tel.: +420 597 321 364, e-mail: miroslav.rosmanit@vsb.cz.
[2] Associate Professor, dr., ir., Technische Universiteit Eindhoven, Department of Architecture, Building and Planning, P.O. Box 513, 5600 MB Eindhoven, tel.: +31 402 472 331, e-mail: m.c.m.bakker@bwk.tue.nl.

For plates with initial imperfections the stress distribution is non-uniform from the onset of loading. In this paper, it is assumed that the plate has a sinusoidal initial imperfection, with the maximum imperfection w_0 occurring at the center of the plate, see Fig. 3.

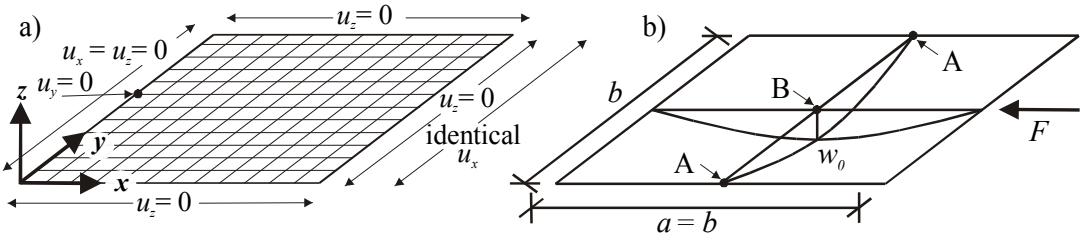

Fig. 2: Schematic view of numerical model: a) Boundary conditions;
b) Initial imperfection, load, measures and location of points A and B.

In this paper the following results will be discussed as functions of the out-of-plane deflection w at the center of the plate, where w is the total out-of-plane deflection at the center of the plate, including the initial imperfection w_0:

- the load F or average stress in x-direction: $\sigma_{x;av} = F/(bt)$;
- the axial shortening u or the average strain in x-direction: $\varepsilon_{x;av} = u/a$;
- membrane stresses $\sigma_{x;A}$ and $\sigma_{x;B}$ in the x-direction at points A and B;
- membrane stress $\sigma_{y;B}$ in the y-direction at point B;

These results can be made dimensionless, by using the buckling stress

$$\sigma_{cr} = \frac{K\pi^2 D}{b^2 t} \tag{1}$$

from which we can define the critical strain

$$\varepsilon_{cr} = \frac{\sigma_{cr}}{E} \tag{2}$$

the critical axial shortening

$$u_{cr} = \varepsilon_{cr} a = \frac{\sigma_{cr} a}{E} \tag{3}$$

and the critical load

$$F_{cr} = bt\sigma_{cr} \tag{4}$$

In these equations D is the plate flexural rigidity factor:

$$D = \frac{Et^3}{12\left(1-\nu^2\right)} \tag{5}$$

t is the plate thickness, a and b are the length and width of the plate (for a square plate $a = b$), E is the modulus of elasticity and K is the buckling coefficient.

In the following first a small-deflection solution summarized by Rhodes [2] and a large-deflection solution given by Williams and Walker [3] are discussed. Then two new solutions are proposed: a modified large-deflection solution which is consistent with the small-deflection solution and a modified strip model based on the strip model of Calladine [4]. The results of these four different solutions are compared to the results of a parameter study with the finite element program ANSYS. Final results can be used to determine the failure loads of compressed square plates. Finally some remarks are made on the effective width method which is often used in the analysis of plate – see Appendix.

2 SMALL-DEFLECTION SOLUTION

The elastic post-buckling behavior of thin plates with initial imperfections is governed by Marguerre's equations [5]. Approximate analytical solutions for these equations can be found by postulating a form for the out-of-plane deflections *w*. At loads below about twice the buckling load the assumption of an unchanging buckled form gives results of engineering accuracy. According to Rhodes [2] the solution based on an unchanging sinusoidal buckling shape can be described by the following equations:

$$\frac{F}{F_{cr}} = \frac{\sigma_{x;av}}{\sigma_{cr}} = (1 - \frac{w_0}{w}) + A_F \eta \qquad \text{with} \qquad A_F = \frac{A}{K}\frac{E^*}{E} \tag{6}$$

$$\frac{u}{u_{cr}} = \frac{\varepsilon_{x;av}}{\varepsilon_{cr}} = (1 - \frac{w_0}{w}) + A_u \eta \qquad \text{with} \qquad A_u = \frac{A}{K} \tag{7}$$

$$\frac{\sigma_{x;A}}{\sigma_{cr}} = (1 - \frac{w_0}{w}) + A_{\sigma x;A} \eta \qquad \text{with} \qquad A_{\sigma x;A} = \frac{A}{K}\frac{E^*}{E} \Big/ \frac{\partial \sigma_{x;av}}{\partial \sigma_{x;A}} \tag{8}$$

where:

$$\eta = \left(\frac{w}{t}\right)^2 - \left(\frac{w_0}{t}\right)^2 \tag{9}$$

A is a coefficient, E^* is an effective Young's modulus and the ratio $\frac{\partial \sigma_{x;av}}{\partial \sigma_{x;A}}$ is a partial variation of the average stress $\sigma_{x;av}$.

Rhodes gives values for the coefficients K, A, $\frac{E^*}{E}$ and $\frac{\partial \sigma_{x;av}}{\partial \sigma_{x;A}}$ depending on the ratio $e = a/b$ of the buckle half width a and the plate width b of the plate. For the case $e = 1$ (square plates), he gives the following values for a simply supported plate with stress-free unloaded edges – Table 1. These values are valid for Poisson's ratio $\nu = 0.3$. The resulting A_F, A_u and $A_{\sigma x;A}$ values are given in Table 4.

Table 1: Coefficients given by Rhodes:

$K = 4$	$A = 2.31$	$\frac{E^*}{E} = 0.408$	$\frac{\partial \sigma_{x;av}}{\partial \sigma_{x;A}} = 0.26$

Rhodes did not give solutions for the membrane stresses $\sigma_{x;B}$ and $\sigma_{y;B}$. Using the solution of the Marguerre equations given in Murray [6] it can be derived [7] that:

$$\frac{\sigma_{x;B}}{\sigma_{cr}} = (1 - \frac{w_0}{w}) + A_{\sigma x;B} \eta \tag{10}$$

$$\frac{\sigma_{y;B}}{\sigma_{cr}} = A_{\sigma y;B} \eta \tag{11}$$

The thus determined $A_{\sigma x;B}$ and $A_{\sigma y;B}$ values are given in Table 4.

3 LARGE-DEFLECTION SOLUTION

For loads larger than about twice the buckling load the changes in the buckling form must be accounted for. Williams and Walker [3] gave an explicit solution for the elastic large-deflection analysis of compressed plates. The two-term format of their expressions is based on the perturbation approach, but the value of the constants in these expressions has been determined from numerical simulations (using the finite difference method).

Their solution takes the following form:

$$A_w^{W\&W}\phi + B_w^{W\&W}\phi^3 = \sqrt{\eta} \tag{12}$$

in which

$$\phi = \sqrt{\frac{F}{F_{cr}} - 1 + \frac{w_0}{w}} \tag{13}$$

$$\frac{u}{u_{cr}} = \frac{F}{F_{cr}} + A_u^{W\&W}\eta + B_u^{W\&W}\eta^2 \tag{14}$$

$$\frac{\sigma_{x;A}}{\sigma_{cr}} = \frac{F}{F_{cr}} + A_{\sigma x;A}^{W\&W}\eta + B_{\sigma x;A}^{W\&W}\eta^2 \tag{15}$$

$$\frac{\sigma_{x;B}}{\sigma_{cr}} = \frac{F}{F_{cr}} + A_{\sigma x;B}^{W\&W}\eta + B_{\sigma x;B}^{W\&W}\eta^2 \tag{16}$$

$$\frac{\sigma_{y;B}}{\sigma_{cr}} = A_{\sigma y;B}^{W\&W}\eta + B_{\sigma y;B}^{W\&W}\eta^2 \tag{17}$$

For a square plate with simply supported edges, subjected to uniaxial compression with the unloaded edges stress free, Williams and Walker [3] give the following values for the coefficients (valid for $\nu = 0.3$):

Table 2: Coefficients given by Williams and Walker – large deflections:

$A_w^{W\&W} = 2.157$ and $B_w^{W\&W} = 0.010$	
$A_u^{W\&W} = 0.341$ and $B_u^{W\&W} = 0.013$	$A_{\sigma x;A}^{W\&W} = 0.628$ and $B_{\sigma x;A}^{W\&W} = 0.010$
$A_{\sigma y;B}^{W\&W} = -0.201$ and $B_{\sigma y;B}^{W\&W} = 0.016$	$A_{\sigma x;B}^{W\&W} = -0.383$ and $B_{\sigma x;B}^{W\&W} = 0.011$

It was found that eqs. (12) to (16) can be rewritten in a format similar to eqs. (6) to (10).

$$\frac{F}{F_{cr}} = \frac{\sigma_{x;av}}{\sigma_{cr}} = (1 - \frac{w_0}{w}) + A_F\,\eta + B_F\,\eta^2 \tag{18}$$

$$\frac{u}{u_{cr}} = \frac{\varepsilon_{x;av}}{\varepsilon_{cr}} = \left(1 - \frac{w_0}{w}\right) + A_u\eta + B_u\eta^2 \tag{19}$$

$$\frac{\sigma_{x;A}}{\sigma_{cr}} = \left(1 - \frac{w_0}{w}\right) + A_{\sigma x;A}\eta + B_{\sigma x;A}\eta^2 \tag{20}$$

$$\frac{\sigma_{x;B}}{\sigma_{cr}} = \left(1 - \frac{w_0}{w}\right) + A_{\sigma x;B}\eta + B_{\sigma x;B}\eta^2 \tag{21}$$

$$\frac{\sigma_{y;B}}{\sigma_{cr}} = A_{\sigma y;B}\eta + B_{\sigma y;B}\eta^2 \qquad (17) \approx (22)$$

The resulting A and B values are given in Table 4.

Williams and Walker [3] also gave a one-term perturbation solution which is accurate enough for design loads up to about 1.5 times the critical load. The general form of the explicit expressions is the same as given in eqs. (12) – (17), except that the second term involving coefficient B is omitted. Unfortunately the coefficients A have to be changed as follows:

Table 3: Coefficients given by Williams and Walker – small deflections:

$A_w^{W\&W} = 2.158$	
$A_u^{W\&W} = 0.347$	$A_{\sigma x;A}^{W\&W} = 0.633$
$A_{\sigma y;B}^{W\&W} = -0.193$	$A_{\sigma x;B}^{W\&W} = -0.378$

Because the results from the one-term perturbation solution are less accurate then the small-deflection solution we will follow only the two-term perturbation solution in this paper. Nevertheless the resulting *A* and *B* values are given in Table 4.

4 MODIFIED LARGE-DEFLECTION SOLUTION

In the perturbation approach by Williams and Walker [3], both the coefficients $A^{W\&W}$ and $B^{W\&W}$ were determined from the results of numerical solutions. In this paper it is proposed to take the coefficients *A* equal to the coefficients determined in the small-deflection solution of the Marguerre equations, and fitting the coefficient *B* to the results of numerical simulations, using the format of eqs. (18) to (22) instead of (12) to (17). The resulting coefficients are given in Table 4. The coefficients *B* where fitted for $w_0 = t$ and $F/F_{cr} = 3.0$, because it was found that these specific values yield the best results [7].

5 MODIFIED STRIP MODEL

Calladine [4] used a simple two-element model to represent the behavior of the plate (see Fig. 3). In this model there are two edge strips with a total width b_{ed} that always remain straight, and one central strip with a width $b_{ce} = b - b_{ed}$ which behaves like a classical Euler column (i.e. it buckles at constant stress, equal to the buckling stress σ_{cr} of the plate).

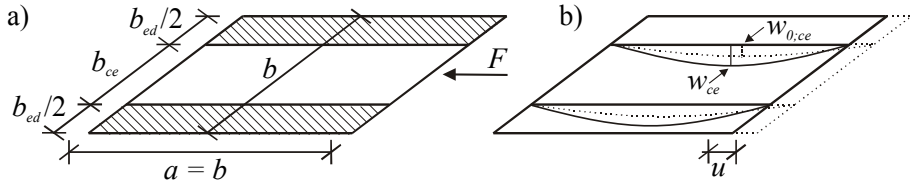

Fig. 3: a) Strip model of the compressed plate by Calladine [4].
b) Deformed strip model of the compressed plate by Calladine [4].

According to this model the total load carried by the plate can be calculated as:

$$F = b_{ed}\sigma_{ed}t + (b - b_{ed})\sigma_{ce}t \tag{23}$$

This formula can also be written as:

$$\frac{F}{F_{cr}} = \frac{\sigma_{x;av}}{\sigma_{cr}} = \frac{b_{ed}}{b}\frac{\sigma_{ed}}{\sigma_{cr}} + \frac{b - b_{ed}}{b}\frac{\sigma_{ce}}{\sigma_{cr}} \tag{24}$$

The strain of the central strip can be calculated as the sum of the elastic compressive strain and the geometric strain ε_g:

$$\frac{\varepsilon_{ce}}{\varepsilon_{cr}} = \frac{\sigma_{ce}}{E\varepsilon_{cr}} + \frac{\varepsilon_g}{\varepsilon_{cr}} = \frac{\sigma_{ce}}{\sigma_{cr}} + \frac{\varepsilon_g}{\varepsilon_{cr}} \tag{25}$$

where ε_g is calculated from the shortening *u* of the central strip due to out-of-plane deflections:

$$\varepsilon_g = \frac{u}{a} = \frac{\pi^2(w_{ce}{}^2 - w_{0;ce}^2)}{4a^2} \tag{26}$$

The central strip behaves likes an Euler column, so that the imperfection amplification factor $\xi = w_{ce} / w_{0;ce}$ can be determined as:

$$\xi = \frac{n}{n+1} \qquad \text{with} \qquad n = \frac{\sigma_{ce}}{\sigma_{cr}} \tag{27}$$

Eq. (27) can be used to calculate the stress in the central strip as a function of the out-of-plane deflection of the plate:

$$\frac{\sigma_{ce}}{\sigma_{cr}} = (1 - 1/\xi) = 1 - \frac{w_{0;ce}}{w_{ce}} \tag{28}$$

Calladine [4] assumed that the maximum lateral deflections w and w_0 of the plate are equal to the maximum lateral deflections w_{ce} and $w_{0;ce}$ of the central strip. In this paper it will be assumed that the maximum deflection of the central strip can be written as:

$$w_{ce} = \sqrt{C_w}\, w \tag{29}$$

and the maximum initial deformation of the central strip can be written as:

$$w_{0;ce} = \sqrt{C_w}\, w_0 \tag{30}$$

Using eqs. (23) and (28) to (30), eq. (25) can be rewritten to give:

$$\frac{\varepsilon_{ce}}{\varepsilon_{cr}} = (1 - \frac{w_0}{w}) + \frac{C_w 3 \cdot (1-\nu^2) b^2}{a^2 K} \eta \tag{31}$$

It can be shown [7] that for elastic edge strip and elastic central strip behavior the modified strip model and the small-deflection model give identical strains if:

$$C_w = \frac{A a^2}{3(1-\nu^2) b^2} \tag{32}$$

Compatibility requires that the strain in the edge strip equals the strain in the central strip:

$$\varepsilon_{ed} = \varepsilon_{ce} = \varepsilon_{x;av} \tag{33}$$

The stress in the edge strip can be calculated as:

$$\sigma_{ed} = E \varepsilon_{ed} \tag{34}$$

Using eqs. (28) to (34), eq. (24) can be written as:

$$\frac{F}{F_{cr}} = \left(1 - \frac{w_0}{w}\right) + \frac{b_{ed}}{b} \frac{A}{K} \eta = \left(1 - \frac{w_0}{w}\right) + A_F \eta \tag{35}$$

Comparing eq. (34) with eq. (6) it can be seen that these two equations give identical results when:

$$\frac{b_{ed}}{b} = \frac{E^*}{E} = \frac{A_F}{A_u} \tag{36}$$

where the coefficients A_F and A_u should be taken from the small-deflection solution.

The modified strip model can also be used in the large-deflection range by using eq. (19) instead of eq. (7) to determine the strains, resulting in:

$$\frac{F}{F_{cr}} = \left(1 - \frac{w_0}{w}\right) + \frac{b_{ed}}{b} \left(A_u \eta + B_u \eta^2\right) \tag{37}$$

Eqs. (37) and (18) give identical results if:

$$\frac{b_{ed}}{b} = \frac{A_F \eta + B_F \eta^2}{A_u \eta + B_u \eta^2} \tag{38}$$

where the coefficients A and B should be taken from the modified large-deflection solution.

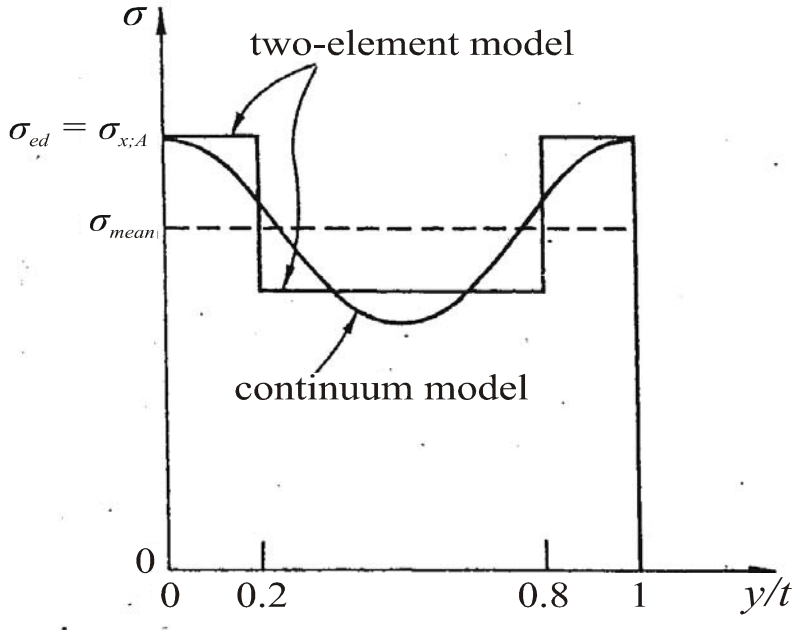

Fig. 4: Model of stress distribution over the central cross section (Calladine [4]). The stresses at the edges of the plate, and the mean stress in the plate, are the same for both continuum and two-element models.

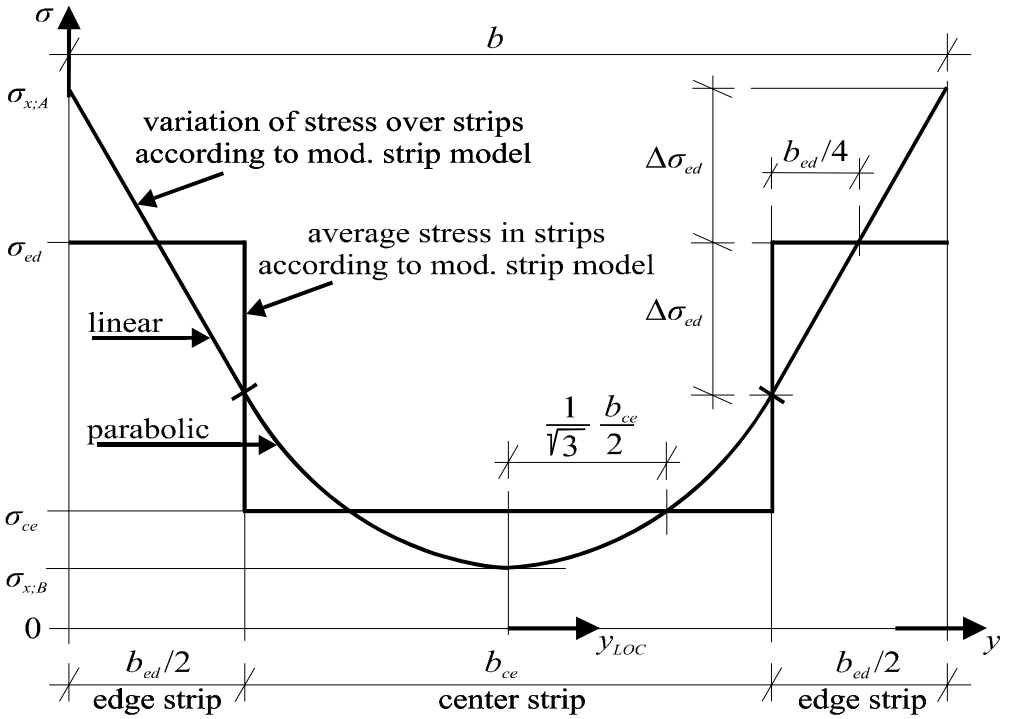

Fig. 5: Two models of stress distribution (idealized) over the central cross section.

Calladine assumed that the stress in the edge strip equals the stress at the edges of the plate ($\sigma_{ed} = \sigma_{x;A}$), Fig. 4. A more accurate edge stress can be calculated by assuming a linear stress distribution over the edge strip and a parabolic stress distribution in the central strip. By taking σ_{ed} and σ_{ce} equal to the average stress over edge and central strip and requiring that the stresses and the stress gradients are continuous at the border between central strip and edge strip (see Fig. 5), the membrane stresses at the edge and center of the plate can be calculated as [7]:

$$\sigma_{x;A} = \sigma_{ed} + \Delta\sigma_{ed} \tag{39}$$

$$\sigma_{x;B} = \sigma_{ce} - \frac{1}{3}\frac{b_{ce}}{b_{ed}}\Delta\sigma_{ed} \tag{40}$$

with

$$\Delta\sigma_{ed} = \left(\sigma_{ed} - \sigma_{ce}\right) \Big/ \left(1 + \frac{2}{3}\frac{b_{ce}}{b_{ed}}\right) \tag{41}$$

Note that by using this method the stresses can be calculated without knowing the small-deflection solution for stresses, and without curve fitting on stresses. Eqs. (39) and (40) can also be written in the format of the equations for the stresses according to the modified large-deflection model (eqs. (18) and (19)). The resulting A and B values are given in Table 4.

Table 4: The resulting coefficients A and B; comparison of the methods:

variable	***coefficients***	***small-def.*** eqs. (6) - (11), resp. (18) – (22)	***large-def.*** eqs. (18) - (22)	***mod. large-def.*** eqs. (18) - (22)	***mod. strip*** eqs. (18), (19), (39) and (40)
F/F_{cr}	A_F	0.2356 (0.2147)*	0.2149	0.2356	
	B_F	0	$-0.4283.10^{-3}$	$-0.3137.10^{-2}$	
u/u_{cr}	A_u	0.5775 (0.5617)*	0.5559	0.5775	
	B_u	0	$0.1257.10^{-1}$	$0.7799.10^{-2}$	
$\sigma_{x;A}/\sigma_{cr}$	$A_{\sigma x;A}$	0.9062 0.9025** (0.8477)*	0.8429	0.9062	0.8710
	$B_{\sigma x;A}$	0	$0.9572.10^{-2}$	$-0.2608.10^{-2}$	$0.5223.10^{-2}$
$\sigma_{x;B}/\sigma_{cr}$	$A_{\sigma x;B}$	-0.1676** (-0.1633)*	-0.1681	-0.1676	-0.1420
	$B_{\sigma x;B}$	0	$0.1057.10^{-1}$	$0.4489.10^{-2}$	$-0.5189.10^{-2}$
$\sigma_{y;B}/\sigma_{cr}$	$A_{\sigma x;B}$	-0.2218** (-0.1930)*	-0.2010	-0.2218	-
	$B_{\sigma x;B}$	0	$-0.1600.10^{-1}$	$-0.1213.10^{-1}$	-

* For completeness' sake - brackets values are coefficients according to William and Walker [3] for one-term perturbation solution.

** The coefficients derived from Marguerre's equations for a rectangular plate with initial dishing, according to Murray [7].

6 FINITE ELEMENT SIMULATIONS

With the finite element program ANSYS 8.1 a numerical parameter study has been carried out. Using eqs. (1), (2), (3), (4), (27) and (28) it can be showed that for elastic calculations only one specific geometry of compressed plate (with one critical stress) is needed. Therefore the plate length and width, plate thickness, Young's modulus and Poisson's coefficient were kept constant in the parameter study: $a = b = 99.8$ mm, $t = 0.7$ mm, $E = 210000\text{N/mm}^2$, $\nu = 0.3$; resulting in a critical stress $\sigma_{cr} = 37.5\ \text{N/mm}^2$.

All boundary conditions, axis convention and the specific points on the plate are presented in fig.3. The used initial imperfections were $0.01t$, $0.1t$, $0.25t$, $0.5t$, $1.0t$, $1.5t$ and $2.0t$. In the model rectangular elements Shell43 were used. The element has six degrees of freedom at each node: translations in the nodal x-, y-, and z-directions and rotations along the nodal axes. The deformation shapes are linear in both in-plane directions. The mesh density for each plate was 40 x 40 elements. In the calculations the effect of large deformations was included. The numerical analyses were performed for loads up to three times the buckling load.

7 DISCUSSION

Graphical and numerical comparisons a representative selection of results is shown in Fig. 6 to 9 and at Table 5; for more results see [7]. The comparison of results shows that the modified large-deflection method gives the most accurate results for the ratio's F/F_{cr} and u/u_{cr}. For small imperfections the small-deflection solution gives results within 5 % error for loads up to about twice the buckling load, but for large initial imperfections the 5 % error occurs at lower loads. With respect to the membrane stresses $\sigma_{x;A}$, it is surprising to see that the small-deflection solution gives better results than the large-deflection solution, even for large initial imperfections and/or large deflections. The modified large-deflection solution does not really improve the small-deflection solution; the modified strip method is slightly less accurate. The accuracy of the membrane stress $\sigma_{x;B}$ is less than the accuracy of the membrane stress $\sigma_{x;A}$, for all models, and deteriorates with increasing initial imperfection.

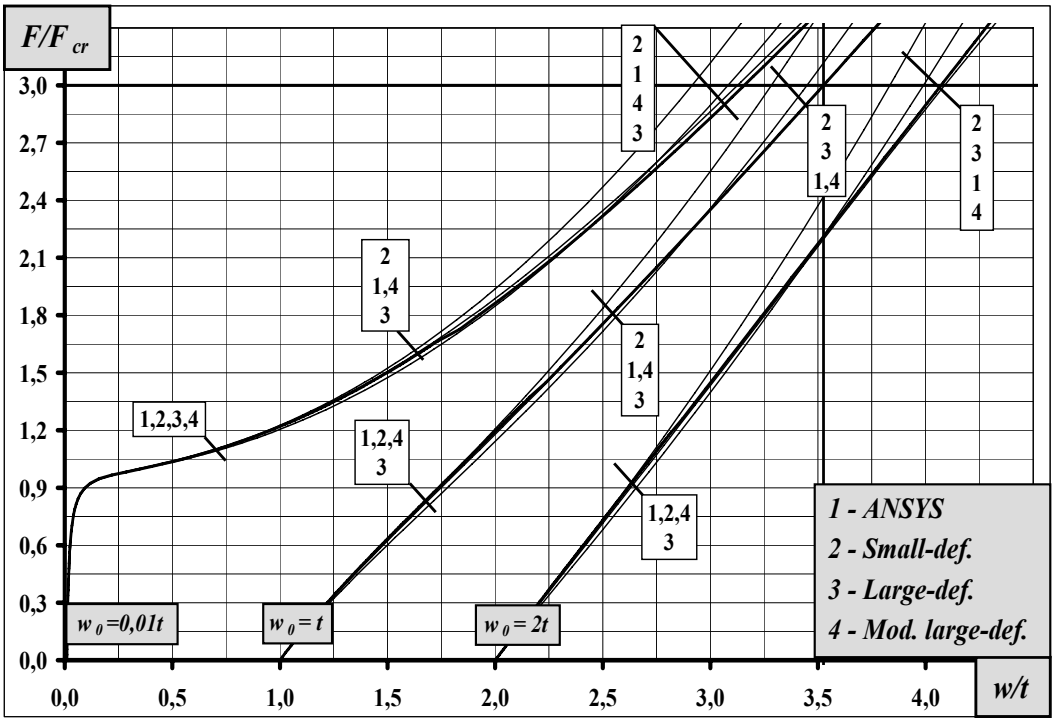

Fig. 6: Comparison of theories: F/F_{cr} and w/t relation.

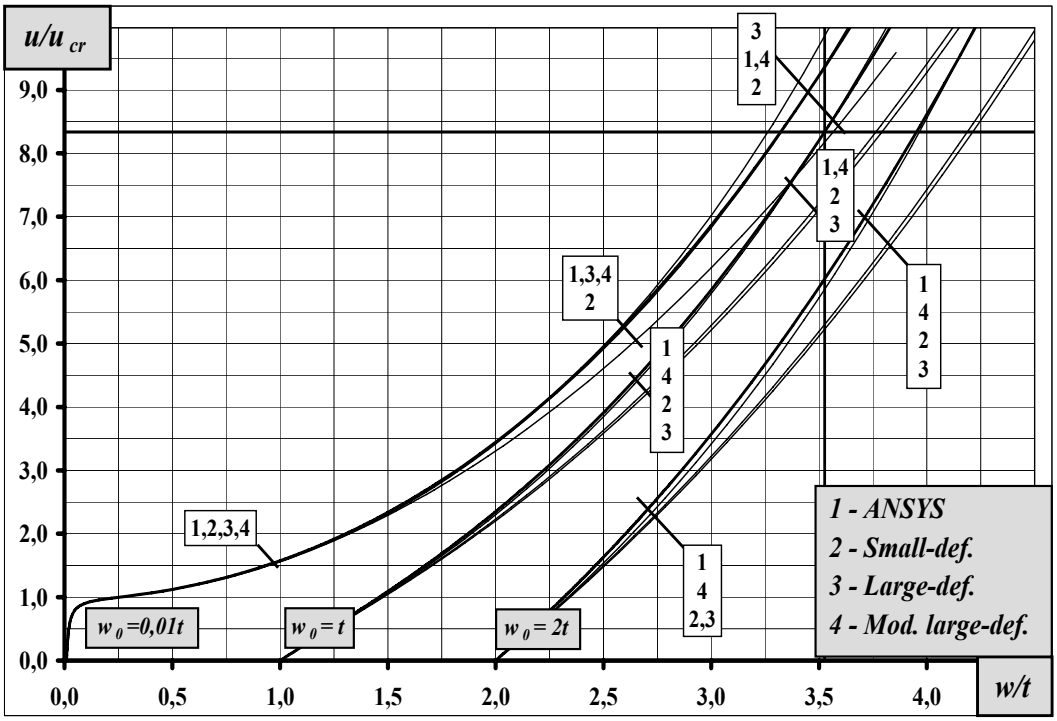

Fig. 7: Comparison of theories: $\sigma_{x;A}/\sigma_{cr}$ and w/t relation.

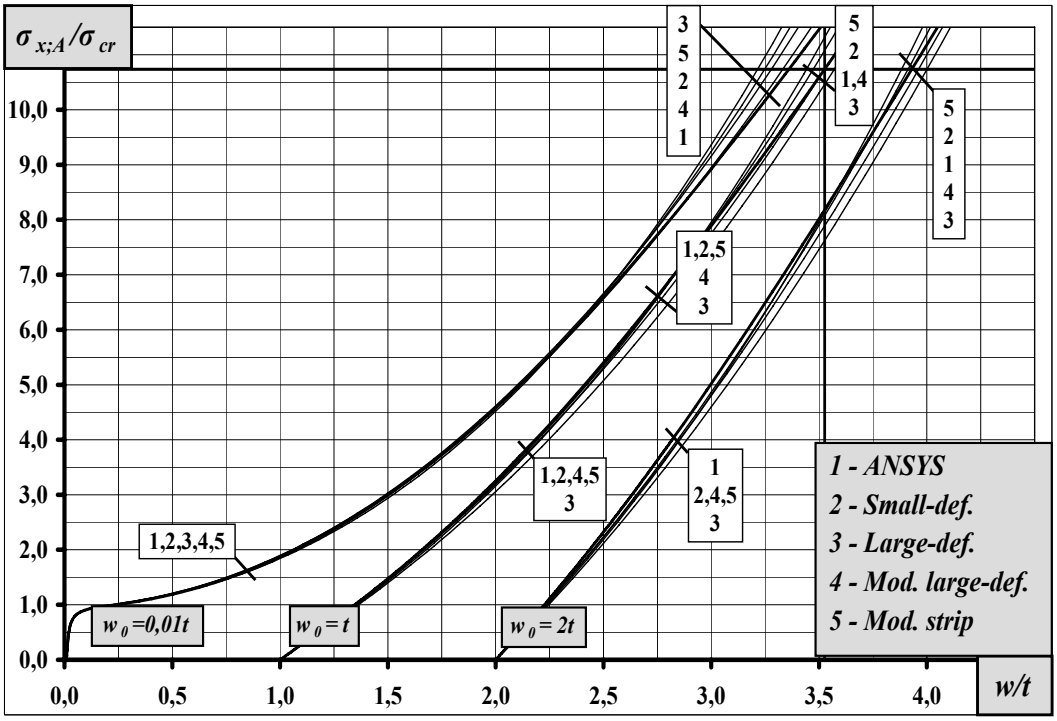

Fig. 8: Comparison of theories: F/F_{cr} and w/t relation.

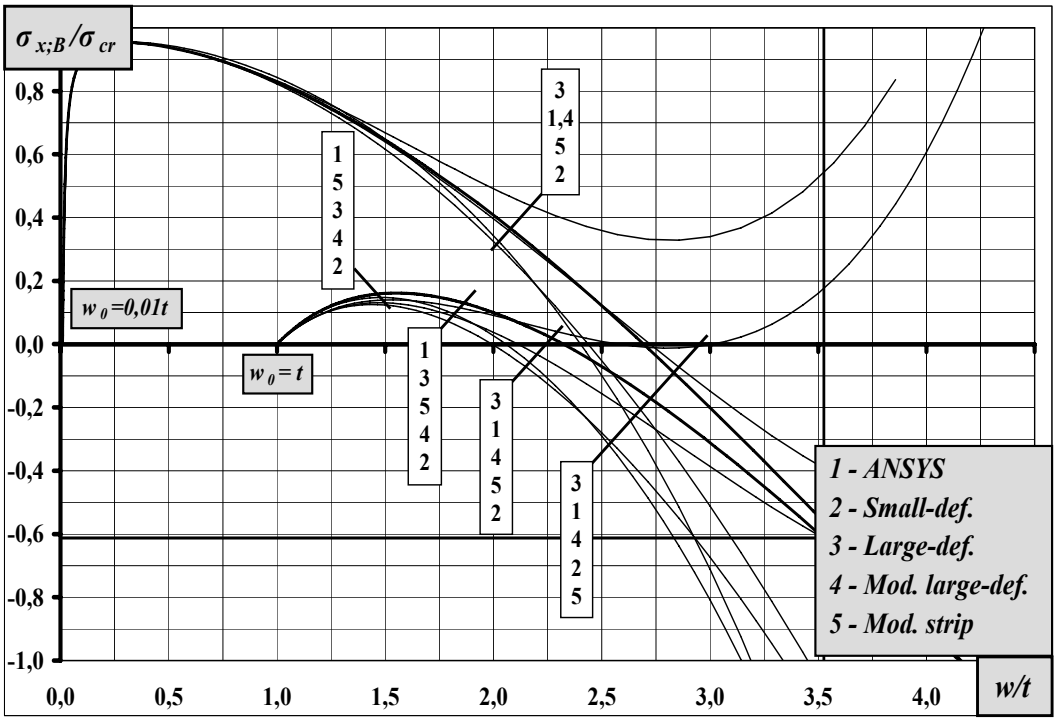

Fig. 9: Comparison of theories: $\sigma_{x;B}/\sigma_{cr}$ and w/t relation.

Table 5: Comparison of theories: The ratio's F/F_{cr} when the first 5 % error occurs – safe validity of the theory.

variable		*theory method*	*initial deflection*						
			0.01*t*	**0.10*t***	**0.25*t***	**0.50*t***	**1.00*t***	**1.50*t***	**2.00*t***
F/F_{cr} according to first 5 % error	F/F_{cr}	*small-def.*	2.16	2.14	2.09	2.03	1.90	1.77	1.63
		large-def.	3.00	3.00	3.00	3.00	3.00	3.00	3.00
		mod. large-def.	3.00	3.00	3.00	3.00	3.00*	3.00*	3.00*
	u/u_{cr}	*small-def.*	2.10	2.05	1.95	1.76	1.20	0.35	0.00
		large-def.	3.00	1.77	1.66	1.42	0.80	0.00	0.00
		mod. large-def.	3.00	3.00	3.00	3.00	3.00	3.00	3.00*
	$\sigma_{x;A}/\sigma_{cr}$	*small-def.*	3.00	3.00	3.00	3.00	3.00	3.00	3.00
		large-def.	2.91	3.00	3.00	3.00	0.48	0.00	0.00
		mod. large-def.	3.00	3.00	3.00	3.00	3.00	3.00	3.00
		mod. strip	3.00	3.00	3.00	2.99	2.95	2.94	2.96*
	$\sigma_{x;B}/\sigma_{cr}$	*small-def.*	1.49	1.39	1.20	0.82	0.00	0.00	0.00
		large-def.	1.54	1.48	1.40	1.30	0.00	0.00	0.00
		mod. large-def.	2.38	2.38	1.58	1.02	0.00	0.00	0.00
		mod. strip	1.71	1.63	1.48	1.21	0.50	0.00	0.00

* When the first 5 % error does not occur in the ratio $F/F_{cr} = 3.0$, then it is 3.0.
Although errors are more than 5 % during the first part of the range observed, they are less than 5 % for the most relevant part (at least $1.14 < F/F_{cr} < 3.00$).

8 CONCLUSIONS

By rewriting the equations of the large-deflection solution given by Williams and Walker [3] in a format similar to the format of the small-deflection solution given by Rhodes [2] these equations become easier to use. A more consistent large-deflection solution can be found by using the coefficients A from the small-deflection model, and fitting only the coefficients B to the results of finite element simulations. The thus determined modified large-deflection solution is more accurate than the large-deflection solution and gives results of engineering accuracy for the ratios F/F_{cr}, u/u_{cr} and $\sigma_{x;A} / \sigma_{cr}$ for loads up to three times the buckling load, and initial imperfections up to two times the plate thickness. For the ratios $\sigma_{x;B} / \sigma_{cr}$ and $\sigma_{y;B} / \sigma_{cr}$ engineering accuracy is obtained for smaller load ranges, which rapidly decrease with increasing initial imperfection.

The modified strip model, based on the strip model by Calladine [4] is identical to the modified large-deflection solution, in the prediction of the ratios F/F_{cr} and u/u_{cr}. Using this model membrane stresses in point A and B can be calculated without fitting coefficients to stress results from numerical simulations. As such, the modified strip model can presumably play an important role in future web-crippling design rules. Note that this method does not give results for moments and for stresses $\sigma_{y;B}$. However, in the small-deflection range moments can be calculated from the small-deflection solution. Membrane stresses $\sigma_{y;B}$ are very small compared to $\sigma_{x;B}$ and do not influence the failure behavior of the plate very much.

It should be checked whether the proposed modified large-deflection method and modified strip model can also be used for other plate geometries, and other boundary conditions.

NOTATION

A_i, B_i	coefficients
D	plate flexural rigidity factor
E	Young's modulus of elasticity
E^*	effective Young's modulus of elasticity by Rhodes [2]
F	load – compression longitudinal force
F_{cr}	critical load
K	buckling coefficient
a, b	plate length/width; for a square plate $a = b$
b_{ce}, b_{ed}	width of the centre respectively edge strip
t	plate thickness
u, u_{cr}	axial shortening respectively critical axial shortening
w, w_0	total respectively initial out-of-plane deflection at the centre of the plate
ε_{ce}, ε_{ed}	average strain at centre respectively edge strip according to σ_{ce}, σ_{ed}
ε_{cr}	critical strain of the plate
ε_g	geometric strain
$\varepsilon_{x;av}$	average strain in x-direction
η	second degree relation of w_0 and w
υ	Poisson's ratio
ξ	imperfection amplification factor
σ_{ce}, σ_{ed}	average membrane stress at centre respectively edge strip
σ_{cr}	critical stress of the plate
$\sigma_{i;j}$	membrane stress on direction i at point j
$\sigma_{x;av}$	average stress in x-direction

APPENDIX - EFFECTIVE WIDTH APPROACH

Von Karman's approach

The term 'effective width' has been used for many years in the description of plate post-buckling behavior. A large series of compression tests on plates of various materials showed that after buckling a plate behaves as if only part of its width is effective in carrying load. The maximum stress occurs at the plate edges while the membrane stresses near the heavily buckled plate centre are relatively small. This phenomenon was investigated theoretically by von Karman [8] who obtained the first effective expression:

$$\int_0^b \sigma \, dx = b_{eff} \sigma_{\max} \tag{42}$$

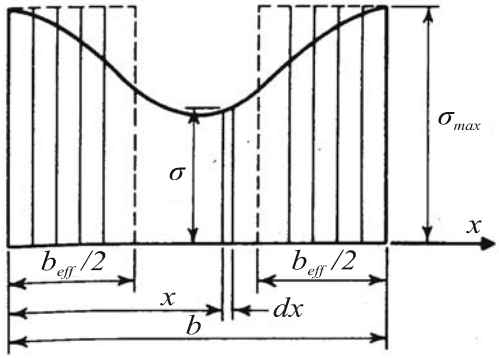

Fig. 10: Effective width of stiffened compression plate – model of von Karman [8].

In this approach it is assumed that the total load is carried by a fictitious effective width b_{eff}, subjected to a uniformly distributed stress equal to the edge stress σ_{max}, as shown in Fig. 10. In this scheme the edge zones became narrowed as the total load increased, and the central zone carried zero stress. Von Karman assumed that the effective width b_{eff} represents a particular width of the plate which just buckles when the compressive stress reaches the yield point. This assumption resulting in (valid for plates without initial imperfections):

$$b_{eff} = C t \sqrt{\frac{E}{f_y}} = 1.9 t \sqrt{\frac{E}{f_y}} \tag{43}$$

where f_y is the yield strength of the material and

$$C = \frac{\pi}{\sqrt{3\left(1-\nu^2\right)}} = 1.9 \tag{44}$$

Eq. (43) can also be written as:

$$\frac{b_{eff}}{b} = \sqrt{\frac{\sigma_{cr}}{f_y}} \tag{45}$$

Winter's approach

Later Winter [9] indicated that eq. (42) is equally applicable to the plates in which the stress is below the yield point, therefore it could be written as:

$$b_{eff} = C t \sqrt{\frac{E}{\sigma_{\max}}} \tag{46}$$

where σ_{max} is the maximum edge stress of the plate.

Winter [10] also found that a straight-line relationship exists between the non-dimensional parameter $(t/b)\sqrt{E/\sigma_{\max}}$ and the term C. The following equation has been developed:

$$C = 1.9\left[1 - 0.475\left(\frac{t}{b}\right)\sqrt{\frac{E}{\sigma_{\max}}}\right] \tag{47}$$

For $(t/b)\sqrt{E/\sigma_{\max}} = 0$, which represent the particular case of extremely large *b/t* ratio with relatively high stress, this formula correspond to von Karman's eq. (43). Using eq. (47), eq. (46) resulting in:

$$b_{eff} = 1.9t\sqrt{\frac{E}{\sigma_{\max}}}\left[1 - 0.475\left(\frac{t}{b}\right)\sqrt{\frac{E}{\sigma_{\max}}}\right] \tag{48}$$

It should be noted that formula (48) implicitly included average influence of initial imperfections.

A long time accumulated experience has indicated that a more realistic equation may be used in the determination of the effective width (Winter [11]):

$$b_{eff} = 1.9t\sqrt{\frac{E}{\sigma_{\max}}}\left[1 - 0.415\left(\frac{t}{b}\right)\sqrt{\frac{E}{\sigma_{\max}}}\right] \tag{49}$$

This equation corresponds to the following relationship:

$$\frac{b_{eff}}{b} = \sqrt{\frac{\sigma_{cr}}{\sigma_{\max}}}\left[1 - 0.22\sqrt{\frac{\sigma_{cr}}{\sigma_{\max}}}\right] \tag{50}$$

Rhodes' approach [2]

Rhodes defined the term effective width in two different forms according to the required purpose – effective width for strength, which describe the maximum stress-deformation behavior, and effective width for stiffness, which describes the load-deformation behavior.

Rhodes defined the effective width for strength $b_{eff;str}$ for uniaxially compressed plates as that width of the fully effective (unbuckled) plate which sustains the same maximum membrane stress as the buckled plate under a given load:

$$\frac{b_{eff;str}}{b} = \frac{\sigma_{av}}{\sigma_{\max}} \tag{51}$$

where σ_{av} is the average membrane stress for a perfect plate. Rhodes assumes the maximum load a plate can withstand is very close to that which causes first membrane yield to occur. Therefore the effective width theory based on the maximum membrane stress is useful in predicting the ultimate strength of a plate.

The effective width for stiffness $b_{eff;stiff}$ for uniaxially compressed plates Rhodes defined as that width of unbuckled plate which sustains the same average strain as the buckled plate for a given load.

$$\frac{b_{eff;stiff}}{b} = \frac{\sigma_{av}}{\sigma_E} \tag{52}$$

where σ_E is an average edge stress. Since the edges of plate do not buckle it can be shown that Hook's rule relates the average edge stress to the average strain and the displacement in the region of the edges. For a uniaxially compressed plate the relationship are:

$$\sigma_E = E\varepsilon_{x;av} = E\frac{u}{a} \tag{53}$$

where $\varepsilon_{x;av}$ is the average strain in the *x*-direction and *u* is the end displacement. Rhodes' expressions for the effective widths explicitly included the influence of initial imperfections, eqs. (6) to (8).

Calladine's approach [4]

Although von Karman concept is inadequate for discussion of the effects of, for example, an initial imperfection, his simple idea does indeed provide a tool for understanding elastic-plastic buckling phenomena of compressed plates. The division of the plate into two distinct regions is closely related to that of von Karman, but the Calladine strip model is differing to von Karman model in one significant detail. Contrary to the von Karman model the edge strips have constant width and the centre of the plate carries the classical buckling stress.

Calladine's expressions also explicitly included the influence of initial imperfections, as was shown in eqs. (26), (28) and (37).

REFERENCES

[1] HOFMEYER, H., ROSMANIT, M., BAKKER, M.C.M.: Parameter study for first-generation sheeting failure using a theoretical and a FE model, 18th International Specialty Conference on Cold-Formed Steel Structures, Orlando, Florida, p. 250-65, 2006.

[2] RHODES, J.: Effective Widths in Plate Buckling, In: Developments in Thin-Walled Structures-1, Edited by Rhodes, J. and Walker, A.C., Applied Science publishers, London, 1982.

[3] WILLIAMS, D.G., WALKER, A.C.: Explicit Solutions for the Design of Initially Deformed Plates Subjected to Compression, Proc. Instn. Civ. Engrs. Part 2.59, pages 763-787, 1975.

[4] Calladine, C.R.: The Strength of Thin Plates in Compression. In: Aspects of the Analysis of the Plate Structures: a volume in honour of Wittrick, W.H. Edited by Dawe, D.J., Horsinton, R.W., Little, A.G., Clarendon Press, Oxford, 1985.

[5] MARGUERRE, K.: Zur Theorie der gekrümmter Platte grosser Form-änderung. Proc. 5th Int. Congress for Applied Mechanics, Cambridge, UK, 1938.

[6] MURRAY, N.W.: Introduction to the Theory of Thin-Walled Structures, Oxford Engineering Science Series 13., Clarendon Press, Oxford, 1986.

[7] ROSMANIT, M. - BAKKER, MCM.: Report on Elastic Post-Buckling Behavior of Uniformly Compressed Plates, Research Report O-2006.02, TU/e Eindhoven, 2006.

[8] Von KARMAN, T., SECHLER, E.E., DONNELL, L.H.: The Strength of Thin Plates in Compression, Transactions ASME, vol. 54, APM 54-5, 1932.

[9] WINTER, G.: Strength of Thin Steel Compression Flanges, (with Appendix), bulletin 35/3, Cornel University Engineering Experiment Station, Ithaca, NY, 1947.

[10] WINTER, G.: Performance of Steel Compression Flanges, preliminary publication, 3rd Congress, The International Association of Bridge and Structural Engineering, Liege, 1948.

[11] WINTER, G.: Commentary on the 1968 Edition of the Specification for the Design of Cold-Formed Steel Structural Members, American Iron and Steel Institute, 1970 ed.

Reviewer: doc. Ing. Tomáš Vraný, CSc.